Environmental Science & Technology

Article

Cite This: Environ. Sci. Technol. 2018, 52, 2375−2384

pubs.acs.org/est

Modeling Net Land Occupation of Hydropower Reservoirs in Norway for Use in Life Cycle Assessment

Martin Dorber,*[,†] Roel May,[‡] and Francesca Verones[†]

[†]Department of Energy and Process Engineering, Norwegian University of Science and Technology (NTNU), Sem Sælands vei 7, 7491 Trondheim, Norway

[‡]Norwegian Institute for Nature Research (NINA), Høgskoleringen 9, 7034 Trondheim, Norway

Supporting Information

ABSTRACT: Increasing hydropower electricity production constitutes a unique opportunity to mitigate climate change impacts. However, hydropower electricity production also impacts aquatic and terrestrial biodiversity through freshwater habitat alteration, water quality degradation, and land use and land use change (LULUC). Today, no operational model exists that covers any of these cause-effect pathways within life cycle assessment (LCA). This paper contributes to the assessment of LULUC impacts of hydropower electricity production in Norway in LCA. We quantified the inundated land area associated with 107 hydropower reservoirs with remote sensing data and related it to yearly electricity production. Therewith, we calculated an average net land occupation of 0.027 m^2·yr/kWh of Norwegian storage hydropower plants for the life cycle inventory. Further, we calculated an adjusted average land occupation of 0.007 m^2·yr/kWh, accounting for an underestimation of water area in the performed maximum likelihood classification. The calculated land occupation values are the basis to support the development of methods for assessing the land occupation impacts of hydropower on biodiversity in LCA at a damage level.

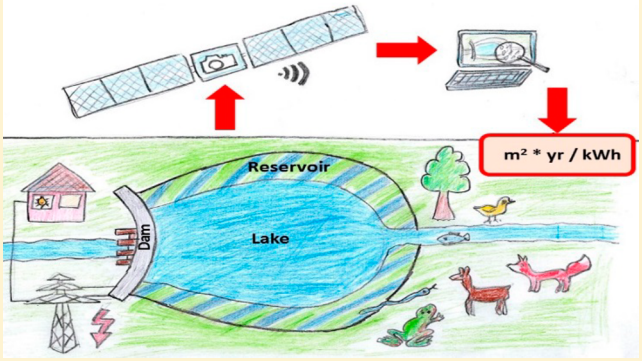

INTRODUCTION

Increasing renewable energy production constitutes a unique opportunity for mitigating climate change impacts.[1] Furthermore, the IPCC has recommended to substantially increase the share of renewable energy in the global energy production.[2] However, even renewable energy sources cause environmental impacts during their life cycle, and these may impact biodiversity.[3−5] Therefore, it is important to assess all relevant impact pathways of renewable energy sources to highlight the main environmental impacts and identify trade-offs between different energy production options and places of operation.

Hydropower electricity production is the largest current source of renewable energy[6] which contributes 16% of the global electricity supply.[7] Its impacts on aquatic and terrestrial biodiversity can be categorized into three main cause-effect pathways.[8] Freshwater habitat alteration potentially affects for example fish, riparian vegetation and macroinvertebrate species,[9−11] water quality degradation can affect (e.g., fish species[12]) and land use and land use change (LULUC) can affect terrestrial and, in part, freshwater flora and fauna.[13−16] All of these pathways may thus lead to local species extinctions and biodiversity loss.[17] However, the three common types of hydropower plants, run-of-river, storage and pumped storage[18] are triggering these impact pathways differently.[8] Run-of-river plants mainly cause freshwater habitat alteration. In contrast, storage and pumped storage hydropower plants affect all of the three mentioned impact pathways.[19]

Concurrently, the IPCCs Special Report on Renewable Energy Sources and Climate Change indicates that there is a need to include long-term environmental consequences from hydropower into current and future projects to identify trade-offs involved with increasing hydropower electricity production.[7] Furthermore, the Norwegian government has pointed out that hydropower electricity production has significant environmental impacts on Norwegian rivers that should be assessed and accounted for.[20]

A particularly suited method for identifying these potential trade-offs between impact pathways is life cycle assessment (LCA). LCA is a commonly used methodology for analyzing the complete environmental impacts of a product or process throughout its life cycle.[21] However, LCA is still developing and can today not assess all relevant biodiversity impacts from hydropower electricity production on a global scale.[8]

In this paper, we address this research gap from a LCA perspective with focus on LULUC, as this is one of the main drivers of global biodiversity loss.[22−24]

Received: October 4, 2017
Revised: December 20, 2017
Accepted: January 12, 2018
Published: January 12, 2018

DOI: 10.1021/acs.est.7b05125
Environ. Sci. Technol. 2018, 52, 2375−2384

Storage and pumped storage hydropower plants, which use dams to store water in reservoirs to allow for flexible electricity production, cause LULUC.[18] Reservoir filling causes LULUC by raising water levels and inundating land.[14] Besides reservoir filling, further LULUC is caused by the construction of infrastructure, including power lines[25] and access roads.[17]

The first step for quantifying the biodiversity impacts of this process in LCA is to assess the land occupation per kWh energy produced, in a comprehensive way. In LCA terms, this corresponds to the life cycle inventory (LCI).[26,27] Because globally underlying environmental parameters, such as topographic and climatic conditions[27] vary considerably,[28,29] spatially explicit LCI information is important.[30,31] However, in LCI databases, such as the largest database, Ecoinvent,[32] spatial land occupation information related to hydropower electricity production is only available for Switzerland and Brazil.[27] Consequently for Norway, one of the top-ten hydropower electricity producers worldwide[33] with more than 95% of domestic power production from hydropower,[34] no spatially explicit land occupation information exist.

In addition, all the currently available hydropower LCI parameters do not account for water area of a potential natural lake prior to the inundation of the reservoir[27,35,36] and represent therefore gross parameters.

However, most of the Norwegian hydropower reservoirs are created by impounding natural lakes,[37] thus applying gross parameters to Norway would consequently lead to an overestimation of LCI values[28] and consequently also of the total impact. However, as natural lake surface area was not recorded at the time when most hydropower reservoirs were constructed,[38] information on natural lake surface areas prior to inundation required for estimating the net land occupation is lacking.(Supporting Information 1 (SI1), section S2).

Remote sensing data provides an opportunity for assessing net land occupation in a spatially explicit manner. Remote sensing data is useful for monitoring actual surface area,[39] as well as wetland identification in general.[40] In addition, case studies on land-use transitions from lakes[41] and lake desiccation,[42] have shown that remote sensing data can be used to calculate natural lake surface area prior to inundation.

To identify land cover types, like water, from satellite images, these studies use the different spectral responses of different land cover types, assessed by the satellite sensor.[43]

Therefore, the first aim of this study was to utilize these case study based approaches in combination with remote sensing data providing global coverage[44,45] to quantify spatially explicit inundated land area values due to the installation of storage hydropower plants in a globally systematically applicable approach.

Due to data availability and the domestic importance of hydropower, we applied our work to Norway to validate the applicability of our approach. The second aim is to use the quantified inundated land area to calculate net reservoir-specific land occupation, in m^2·year per kWh of hydropower electricity produced. Land occupation caused by the construction of associated infrastructure, such as roads and power lines, was not considered in this study. This net land occupation can be directly implemented in LCIs. While beyond the scope of this paper, the presented approach is a crucial step toward quantifying impacts of hydropower electricity production on biodiversity in LCA.

MATERIALS AND METHODS

Inundated Land Area of Hydropower Reservoirs. Constructing hydropower reservoirs by either damming a river or impounding a natural lake leads to an inundated land area (ILA).[37] Maximal ILA [m^2], for each dammed waterbody x, is the difference between the actual reservoir surface area at highest regulated water level (RSA) and the waterbody surface area before dam construction (WSA), both assumed constant over time (eq 1). This assumption is valid on a long-term perspective with no anthropogenic disturbance.[46]

$$\mathrm{ILA}_x = \mathrm{RSA}_x - \mathrm{WSA}_x \quad (1)$$

In this study we used the actual reservoir surface area at highest regulated water level with commissioning year provided by the Norwegian Water Resources and Energy Directorate (NVE),[38] as this database provides the most detailed information for Norway. We estimate waterbody surface area before dam construction using Landsat data[44] with global coverage, and aerial photographs,[45] as described in the following sections.

Origin of the Remote Sensing Data. Satellite images were downloaded from the NASA-USGS Global Land Survey data set (GLS) provided by the public domain of U.S. Geological Survey.[44] The GLS data set is a collection of freely accessible, orthorectified and cloud-minimized Landsat satellite images with global coverage, which has been used to map global forest cover,[47] as well as historical changes of wetlands.[40,48,49]

Due to the age of most hydropower reservoirs in Norway, we used the oldest assembled epoch, the GLS-1975 data set, with Landsat 1−3 images acquired from 1972 to 1983 with a resolution of 60 m.[50] We extracted 32 multispectral images from the GLS-1975 available for Norway, which were not totally covered with ice and snow (SI1, S3). Images were then sorted by satellite and merged in ArcGIS10.3[51] by path. The path describes the orbital track of the satellite from east to west. Consequently, we avoided overlap of images and ensured the use of all extracted images for Norway. As a result, we obtained 13 merged multispectral images, which are path and satellite specific (SI1, S3).

In addition, seven aerial photographs where obtained from the Internet portal Norge i Bilder[45] as additional data source. This platform provides aerial photographs for Norway with a resolution of 0.2 m, dating back to 1937 (SI1, S4).

Quantifying Water Surface Area before Dam Construction. To assess the water surface area before dam construction, the commissioning year of the hydropower reservoirs has to be equal or younger than the exposure year of the remote sensing data. This means that we can potentially assess water surface area before dam construction of hydropower reservoirs with commissioning year equal or after 1936 from aerial photographs and with commissioning year 1972 and after from Landsat images. Additionally, WSA can only be calculated for hydropower reservoirs that were not covered with ice and snow or clouds during the image exposure date, as this makes identification of water surface areas impossible. To calculate water surface area before dam construction from Landsat images, the water body area was identified with an image classification method. To classify land cover types from satellite images two main methods exist: unsupervised and supervised classification.[43] Unsupervised classification aggregates pixels with similar spectral values in clusters, which are then assigned to a land cover type.[40] In the more commonly

DOI: 10.1021/acs.est.7b05125
Environ. Sci. Technol. 2018, 52, 2375−2384

used supervised maximum likelihood classification,[43] land cover types are identified based on user-defined training areas, consisting of area on the satellite image where the land cover type is known.[40] The maximum likelihood classification, has the advantage that with training areas our desired land cover type "water" can be chosen directly, whereas in the unsupervised classification a single cluster may not correspond with the land cover type "water", because one land cover type can be represented by multiple clusters.[40] Therefore, we performed a supervised maximum likelihood classification in ArcGIS10.3[51] to identify water pixels on the Landsat satellite images.

For each merged multispectral image, we created training areas each comprising either a "water" or "non-water" land cover type. Each land cover type was defined by several training areas. The maximum likelihood classification analyzes the pixel values, defined by the spectral reflectance of the pixels in the different spectral bands of the satellite image, of all training areas in each land cover type. The mean and variance of the pixel values in each land cover type is then used to categorize all pixels of the image in the land cover type with the highest probability of a membership.[40] "Water" training areas consisted of areas clearly identified as water on the true color satellite images. These mainly consisted of lakes and, where available, fjord areas. As certainty of water identification increases with lake size, we used the largest lakes available on the image for training. Additionally, we included, if present, fjords, lakes in mountainous areas and lakes containing algae, as they have different spectral reflectances.[40] Nonwater training areas consisted of the land cover types: land, clouds, and ice and snow. These land cover types have different spectral reflectance, and thus improve the correct categorization of these pixels in the right land cover type, avoiding misclassification of water pixels. The amount and size of training areas depended on the land cover types contained by the merged multispectral images. Scatterplots were used to ensure that the spectral reflectance of water and nonwater training areas did not overlap. The maximum likelihood classification was performed with each of the merged multispectral images (SI1, S3). Water surface area before dam construction from Landsat images was calculated with eq 2, using the identified pixels of the land cover type "water".

$$\mathrm{WSA}_x = \mathrm{WP}_x \times \mathrm{PR} \tag{2}$$

Where WP is the number of water pixels of reservoir x on the GLS-1975 image within the boundary of the reservoir at highest regulated water level and PR is the pixel resolution in m^2.

The images from the different Landsat-paths can overlap, thus partly covering the same area (SI1, S3).

As a result, we calculated up to four different water pixel numbers for each hydropower reservoir. In these cases, we used the maximum number of water pixels as final WP_x, assuming representation of the maximum water level of the natural lake (SI2). With the number of water pixels, we calculated water surface area before dam construction and consequently the net land occupation with eq 1, for ice/snow- and cloud-free hydropower reservoirs on the merged multispectral images.

From 11 hydropower reservoirs on aerial photographs, we obtained WSA directly by using the online measurement tool from Norge i Bilder[45] and used eq 1 to calculate the inundated land area. Direct measurement was possible due to image resolution (SI1, S4).

Inundated land area estimates from remote sensing data were based on a planar surface, thereby assuming that the slope of the terrain is always zero. However, inundated land area around reservoirs, which are usually situated in mountainous regions, will most likely not be on a flat surface. Therefore, we tested the effect of slope by also calculating inundated land area with a sloped terrain. However, there was no significant effect of slope, and thus we have not considered the inundated land area with a sloped terrain in this study (SI1, S6).

Land Occupation Modeling for the Life Cycle Inventory. The inundated land area represents a land use change. For land use, LCA distinguishes between land occupation and land transformation. Land occupation is defined as a use of a land area for a certain human-controlled purpose. The recovery to the original state is postponed by a period of time equal to the duration of the occupation process.[52] Land transformation is defined as a change a of land area in line with requirements of a new occupation process. The recovery to the original state is depending on the severity of transformation, the duration of land occupation and the recoverability of the affected terrestrial habitat.[52] For our purpose, we define the land use caused by the inundation of land as land occupation, as the inundation of land occurs over a specific time for a human-controlled purpose. Further, studies have documented a fast geomorphic floodplain change inherent with an ecological recovery after dam removals.[53,54]

The net land occupation LO_x [m^2·yr/kWh] modeled for the LCI (eq 3), relates the inundated land area of each hydropower reservoir x to yearly average electricity production, assuming that the reservoir is only used for hydropower electricity production.

$$\mathrm{LO}_x = \frac{\mathrm{ILA}_x}{\mathrm{ER}_x} \tag{3}$$

ER is the average annual electricity production of hydropower reservoir x in kWh. ILA is the inundated land area of hydropower reservoir $x$in m^2.

As Bakken et al.[28] pointed out that the power production of several hydropower plants could benefit from the creation and regulation of the uppermost hydropower reservoir in a cascade system, we calculated ER for each reservoir x with eq 4:

$$\mathrm{ER}_x = \sum_{m=1}^{m} \frac{\mathrm{RSA}_x}{\sum_{n=1}^{n} \mathrm{RSA}_{x \in z|\mathrm{upstream}}} \cdot E_z \tag{4}$$

RSA is the actual reservoir surface area at highest regulated water level in m^2. n is the number of upstream reservoirs located in Norway connected to hydropower plant z. E is the average annual electricity production at hydropower plant z in kWh. m is the number of hydropower plants located downstream of reservoir x. We received RSA, n, m and average E (between 1981 and 2010) from the Norwegian Water Resources and Energy Directorate (SI2).[38,55] We assumed that this is the average true electricity production in a normal year and is not significantly fluctuating over the years. Average hydropower electricity production in a normal year is calculated as a function of installed capacity and expected annual inflow in a year with normal precipitation.[34] However, for pumped storage plants, which have usually a negative net electricity output,[56] this methodology is not applicable.[27] Therefore, we did not calculate land occupation values for reservoirs directly assigned to a pumped storage hydropower plant with negative net electricity production. Additionally, due to the resolution of the satellite images (60 m), reservoirs with an RSA smaller than

DOI: 10.1021/acs.est.7b05125
Environ. Sci. Technol. 2018, 52, 2375−2384

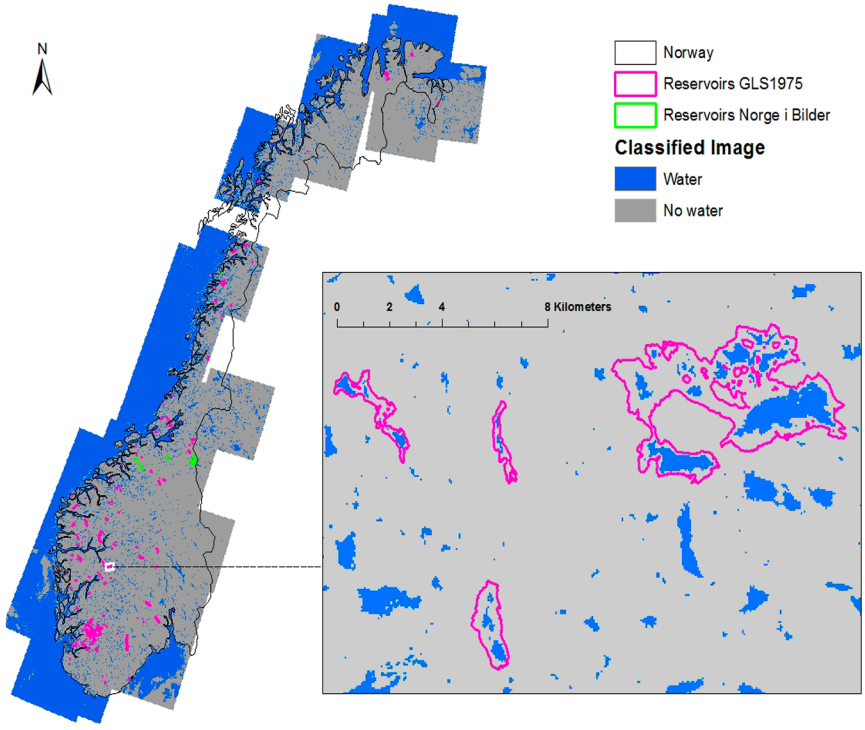

Figure 1. Merged classified image of all 13 Landsat paths, showing water (blue) and nonwater pixels (gray) overlaid with hydropower reservoirs[38] in Norway[58] where inundated land area was quantified from the NASA-USGS Global Land Survey GLS-1975[44] data set (pink) or from aerial photographs from the Internet portal Norge i Bilder[45] (green). The enlarged area shows an example of a more detailed view of the map.

0.5 km^2 were excluded from the calculations and not assigned to a hydropower plant.

Uncertainty of the Land Occupation Calculation. Frazier and Page[57] report that maximum likelihood classification underestimates the amount of water pixels due to mixed pixels, which contain more than one land cover type. In our case, mixed pixels are located at the shore of the reservoirs and contain both water and nonwater land cover types. To assess the uncertainty in the land occupation calculation due to this potential bias, we calculated the water body area of natural lakes with surface area larger than 0.5 km^2 contained by the classified images obtained from the maximum likelihood classification and compared this calculated water body area to the actual natural lake surface area provided by NVE.[38] Here, we assumed that the surface area of natural lakes remains constant over time. We limited our error analyses to Landsat 1 Path 214 and Path 215, as lakes must be manually checked for ice and cloud cover (SI2). We regressed the latter area against the calculated maximum likelihood classification area using a generalized linear model with a quasi-Gaussian distribution to account for the skewness of the data. Based on this model, we estimated, adjusted water surface areas (WSA_{adj}), the subsequent adjusted land occupation (ALO), and associated confidence intervals. In cases where the adjusted land occupation value became negative, due to a larger WSA_{adj} compared to RSA, we set it to zero.

RESULTS

Inundated Land Area of Hydropower Reservoirs. We were able to quantify the inundated land area for 184 of the 265 hydropower reservoirs in Norway that have a commissioning year of 1972 or after (SI1, S2 and SI2). The main reason for not quantifying all hydropower reservoirs with commissioning year of 1972 or after is the fact that many GLS-1975 images were acquired in early May or October[50] when lakes are frozen in Norway making identification of some water surface areas impossible. This was also the main reason for the low number of hydropower reservoirs with quantified ILA in the north (Figure 1).

Total ILA from 1972 up to today is 305.3 km^2 with an average of 1.66 km^2 and ranging from 0.003 km^2 to 63.9 km^2 per hydropower reservoir.

We calculated ILA for 173 hydropower reservoirs from 32 GLS-1975 images[44] covering 13 paths, and ILA for another 11 hydropower reservoirs from 6 aerial photographs.[45] We excluded GLS-1975 images that did not contain any ice- or cloud-free hydropower reservoirs. Therefore, the classified image in Figure 1 contains gaps, despite the fact that GLS-1975 images are available for the whole of Norway.

Land Occupation Modeling for the Life Cycle Inventory. Of the 184 hydropower reservoirs identified on the satellite images and aerial photographs, 73 hydropower reservoirs were excluded from the land occupation calculation due to small surface area (<0.5 km^2) and one because related hydropower plant were not available from NVE.[38] In total, three of the 184 hydropower reservoirs were assigned to a pumped storage hydropower plant, but had to be excluded as their net electricity output was negative.

Consequently 107 hydropower reservoirs of storage power plants (96 from GLS-1975 and 11 from Norge i Bilder), were used to calculate the land occupation with the obtained inundated land area (Figure 2; SI2). Thereof, 100 hydropower reservoirs were only used for hydropower electricity production. Five were also used as recreational dams, one as fishing dam, and one for water supply. The average land

DOI: 10.1021/acs.est.7b05125
Environ. Sci. Technol. 2018, 52, 2375−2384

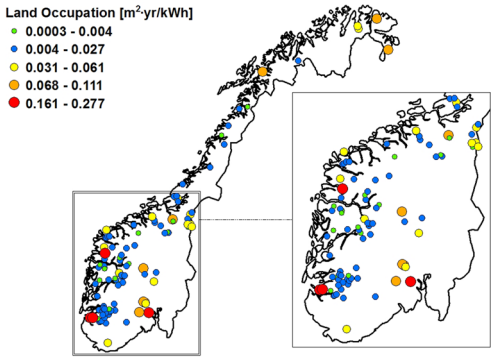

Figure 2. Map showing the land occupation [m^2·yr/kWh] for each hydropower reservoir in Norway.[58] For an easier identification, the inset map shows a more detailed view of southern Norway.

occupation across all investigated hydropower reservoirs was calculated as 0.027 m^2·yr/kWh.

We assessed land occupation for 75% (808 km^2) of the RSA from hydropower reservoirs with commissioning year of 1972 or after in Norway. This represents 13.4% of the total RSA of all hydropower reservoirs in Norway. The 107 hydropower reservoirs have an average annual electricity production of 27.059 GWh, representing 19.6% of the total average annual hydropower electricity produced in Norway between 1981 and 2010.

Land Occupation Uncertainty. For the Landsat 1 Path 214, the natural water surface area (dispersion parameter: 0.077; intercept: −0.303 ± 0.029, $P < 0.001$) was significantly related to the maximum likelihood classification water surface area (1.068 ± 0.011 SD, $P < 0.001$). For the Landsat 1 Path 215, the natural water surface area (dispersion parameter: 0.024; intercept: 0.228 ± 0.013, $P < 0.001$) was significantly related to the maximum likelihood classification water surface area (1.103 ± 0.009 SD, $P < 0.001$). The averaged correction values across both Landsat 1 Paths were used to adjust the water surface area, including 95% confidence intervals (intercept: 0.266 ± 0.022 SD; water surface area: 1.085 ± 0.010 SD). After adjustment, the ratio of the natural to calculated water surface area reduced from 1.40 (95% percentile: 1.04−2.23) to 0.97 (95% percentile: 0.70−1.28); removing underestimation of the water surface area.

In 31 cases, the adjusted land occupation was set to zero, due to a larger WSA_{adj} then RSA, indicating that a natural lake became utilized as reservoir. With this, we calculated an adjusted land occupation with an average of 0.007 m^2·yr/kWh (Figure 3).

Using WSA_{adj} instead of WSA resulted in adjusted land occupation values 2.7−100% smaller than the previous calculated land occupation values. This variation can be explained as the difference between WSA_{adj} and WSA in relation to the ILA. The example of the Reservoir Riskallvatn shows that even if WSA_{adj} is 293% larger (0.24 km^2) than WSA, the difference of adjusted land occupation in relation to land occupation is only 28.9%, because the difference is small in comparison to the previously estimated inundated land area of 0.89 km^2. In contrast, for the Breimsvatn Reservoir, WSA_{adj} is only 110% larger (2.02 km^2) than WSA, but as this value is big in comparison to the previously estimated inundated land area of 2.04 km^2, the difference of adjusted land occupation in relation to land occupation is 98.9%.

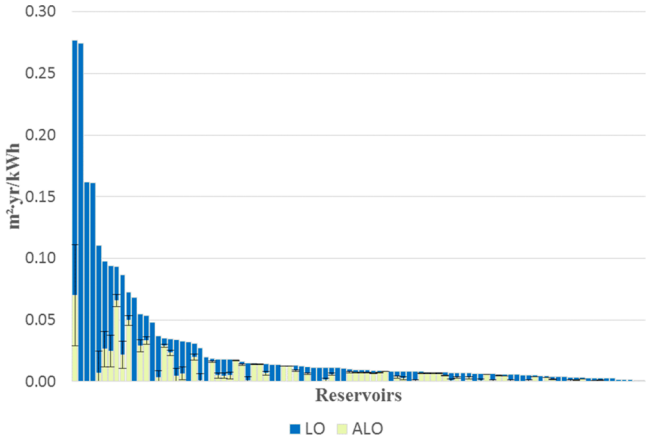

Figure 3. Comparison of land occupation (LO) in blue and adjusted land occupation (ALO) in mint with standard deviation of ALO in black. In 31 cases, the adjusted land occupation was set to zero.

DISCUSSION

Calculating Inundated Land Area from Remote Sensing Data. We performed a supervised maximum likelihood classification on GLS-1975 Landsat MSS images[44] to identify water pixels and showed that it is possible to assess the inundated land area on a reservoir level for the whole of Norway. Even though we used a supervised classification method, unsupervised classification techniques have also been used for wetland classification. Unsupervised classification aggregates pixels with similar spectral values in clusters and the step of defining training areas is therefore not necessary.[40] However, the corresponding step in the unsupervised classification is the assignment of clusters to a land cover type[43] and unsupervised classification for wetlands is only effective when a large number of clusters is used.[40]

Additionally in our case, identifying land cover types of clusters only including small lakes or the border area between land and water on a satellite image with a 60 m resolution would have been almost impossible. In the supervised maximum likelihood classification, we defined our desired land cover type "water" directly by using training areas that were clearly identifiable as water. All pixels were categorized in the land cover type with the highest probability of a membership. This is an advantage in comparison to the unsupervised classification method. The selected supervised maximum likelihood classification was therefore deemed the appropriate classification method for our purpose.[40]

Besides the two main classification methods, the normalized difference water index (NDWI) was developed to quantify open water areas.[59] This index performs best when a middle infrared band is used.[60,61] The Landsat MSS data used in this study, however, does not cover this band. We were therefore not able to use the NDWI in this study. However, the NDWI may be applied when calculating the inundated land area of more recently built hydropower reservoirs from more recent satellite images, containing a middle infrared band.

We used the nonslope corrected inundated land area to calculate the land occupation, as there was no statistically significant difference between slope-adjusted ILA and ILA. However, slope-adjusted ILA was always larger than ILA. For the slope-adjusted ILA we assumed that the slope outside and inside the water body was the same. As this is not always the case, the potential error of this assumption might, however, be

DOI: 10.1021/acs.est.7b05125
Environ. Sci. Technol. 2018, 52, 2375−2384

higher than the quantified effect.[62] As such, we recommend using ILA, as done in this study, and not slope-adjusted ILA, but account for the potential underestimation of ILA (SI1, S5).

Land Occupation Modeling for the Life Cycle Inventory. We calculated a land occupation value for 107 of 1289 hydropower reservoirs in Norway. We thereby calculated a land occupation value for 96 of the 250 hydropower reservoirs that have a commissioning year of 1972 or after, with the GLS-1975 data set. The number of 107 is high, because many images were acquired when lakes are frozen in Norway. Considering that the GLS-1975 is the oldest available satellite image set available,[50] the main limiting factor to assess all hydropower reservoirs in Norway is the image acquisition year. However, our number of 107 reservoirs is much higher than the 52 reservoirs assessed for Switzerland and the one reservoir for Brazil in the existing Ecoinvent database.[27] The average land occupation in our study across all investigated hydropower plants is 0.027 m^2·yr/kWh and is larger than the existing 0.004 m^2·yr/kWh in the Ecoinvent database,[27] despite the fact that we calculated the net land occupation.

When comparing average values it has to be considered that we only calculated a land occupation value for 107 hydropower reservoirs. Further assessment of land occupation values of neglected reservoirs in this study could therefore change the average net land occupation value. However, a more detailed quantification is not possible, as we have applied all the available information regarding inundated land area of Norwegian hydropower reservoirs.

The land occupation varies between 0.0003 m^2·yr/kWh and 0.28 m^2·yr/kWh and therefore 18 reservoir-specific LO values were lower than the Ecoinvent value.[27] The range of our values highlights the importance of site-specific life cycle inventory modeling, even when not all hydropower reservoirs of a country are assessed.

However, further research is needed to asses a land occupation value for hydropower reservoirs with commissioning year of 1972 or before. A promising starting point could be old lake depth maps with lake surface area calculations. The focus of the old analog lake depth maps in Norway[63] was to quantify the depth and water volume to predict ice conditions after a possible regulation. Hence, only depth soundings were conducted as fieldwork, while water surface area estimation is based on the M711 topographic map series.[63] This map series was compiled between 1952 and 1988.[64] Due to this time span, it is not ensured that the estimated water surface area represents the status before the dam construction. Therefore, we did not include this additional information, although it reduced the amount of included hydropower reservoirs.

As impacts of power generation are generally compared per unit of electricity produced,[65−67] we are describing the land occupation per kWh hydropower produced. As the power production of several hydropower plants could benefit from the creation and regulation of the uppermost hydropower reservoir in a cascade system, we used the RSA to reallocate the electricity produced for the land occupation calculation. This assumption might be incorrect, as factors like reservoir volume might also have an influence. However, it is a method to ensure that produced electricity is not double counted.

Seven out of 107 reservoirs used to calculate land occupation are used as multipurpose reservoirs,[38] thus hydropower electricity production is not the only reason causing land occupation. In multipurpose reservoirs the impact should therefore be allocated between use purposes[68] as part of the land occupation should be related to the other purposes. Nevertheless, allocation guidance is still lacking[68] and due to the low number of seven multipurpose reservoirs we have not included an allocation factor. Therefore, our calculated land occupation may overestimate the land occupation for these seven hydropower reservoirs that are used for several purposes.

Due to satellite image resolution, the land occupation is only quantifying the amount of land occupied, but not which type of land cover nor its significance for terrestrial biodiversity or the effect on evaporation rates and the related water consumption. However, when quantifying the land occupation of newly built hydropower reservoirs, newer remote sensing data that have a higher spatial resolution can be used. This higher resolution, for example allows that the habitat quality of the occupied land could be assessed as shown by Zlinszky et al.[69]

Land Occupation Uncertainty. The adjusted average land occupation (0.007 m^2·yr/kWh) is lower than the average land occupation (0.027 m^2·yr/kWh) and therewith closer to the existing 0.004 m^2·yr/kWh in the Ecoinvent database.[27] Furthermore, the adjusted average land occupation varies between 0 and 0.07 m^2·yr/kWh showing the importance of spatially explicit life cycle inventory modeling.

Frazier and Page[57] report that maximum likelihood classification underestimates the amount of water pixels, which is in accordance with our uncertainty analysis, as for both Landsat 1 Path 214 and 215 the maximum likelihood classification water surface area was always smaller than the natural water surface.

An underestimation of approximately 5% for water area classification from Landsat MSS data is reported by Smith.[49] Frazier and Page[57] performed a maximum likelihood classification on Landsat TM data to identify water bodies. For lakes with a surface area of 0.06 to 0.18 km^2 an underestimation of 43.5% was reported and for water bodies with surface areas of 50 m^2 to 0.032 km^2 an underestimation of up to 80%.[57]

These studies confirm that our maximum likelihood classification, with an underestimation of 39% and 36% for natural lakes on Landsat 1 Path 214 and Path 215 with surface areas <1 km^2, performs within the conventional range and that uncertainty is indeed depending on lake surface area. The average underestimation of 8% for natural lakes with surface area >5 km^2 Landsat 1 Path 214 is close to the reported 5% by Smith (SI2).[49]

As the number of mixed pixels decreases with higher image resolution,[40] choosing a higher image resolution presents the best way to reduce mixed pixels and therewith the underestimation of water surface from small lakes. However, this option is not possible for the Landsat 1−3 images used in this study.

In addition, variability in annual electricity production (ER) should be included in the confidence intervals. These data, however, were not available for this study.

Besides methodological uncertainty,[40] which we quantified in this study, seasonal aspects and geolocation error of the GLS-1975[50] are most likely the largest contributors to uncertainty. However, quantification of these uncertainties in a systematic way is difficult. Therefore, they can be only discussed qualitatively in the following section, nevertheless adding an undefined amount of error to our performed error analysis.

To calculate WSA and WSA_{adj} we assumed that natural lakes have a constant surface area over time. This assumption is correct for a long-term perspective with no anthropogenic

DOI: 10.1021/acs.est.7b05125
Environ. Sci. Technol. 2018, 52, 2375−2384

disturbance.[46,70] Nevertheless, water levels of freshwater lakes can have a seasonal fluctuation.[71] These fluctuations can have different amplitudes.[46,70,72] For lake Atnasjøen in Norway an average seasonal fluctuation of approximately 1 m is reported, characterized by spring-floods due to the snowmelt.[73]

The Landsat images used in this study were acquired between 1972 and 1983 and from early May to October or later.[50] They therefore may include both high and low water levels resulting in different waterbody surface areas.

We accounted for high levels, assuming that these represent the natural maximum range of the lake, by using the maximum number of water pixels obtained for each hydropower reservoir to calculate WSA. However, due to the temporal resolution of the Landsat images even the maximum number of water pixels pertain to a period of low water level, leading to an underestimation of WSA and overestimation of LO.

Moreover, the GLS-1975 data set has a geolocation error of maximal 24.9 m in comparison to the GLS-2000.[50] Therefore, RSA and classified GLS-1975 images may be shifted against each other. As a result, counted pixels on the satellite image may not intersect with RSA in reality, resulting in wrong WSA estimates.

Implementation and Use in LCA. The unit of the modeled land occupation is m^2·yr/kWh. This is in accordance with the unit of m^2·years for land occupation in the land use inventory[74] and therefore our net land occupation values calculated for storage hydropower reservoirs are directly implementable in LCI databases.

We assumed that the average annual electricity production is the "true" electricity production in a normal year. In the long term perspective this assumption is indeed correct,[34] therefore the average annual electricity production can be used to calculate the land occupation per kWh produced. This means that our values are designed to calculate the average land occupation over the complete operational phase. They are, however, not applicable for individual years, as this can either lead to over- or underestimation of the average yearly land occupation, because the annual inflow to hydropower reservoirs in Norway has varied from 1990 to 2013 by about 60 TWh. This, for example, caused the variation in the hydropower electricity production in the whole of Norway from 143 TWh in 2000 to 106 TWh in 2003, the latter being a very dry year.[34] However, if the efficiency of the hydropower plants change over time (e.g., due to changes in precipitation patterns), the inventory has to be updated, as this will reduce the land occupation per kWh. Some land occupation inventory parameters are designed to predict future land occupation impacts.[75] In contrast, our calculated land occupation is only representative for the period from 1972 to 1985 and should not be used to quantify the land occupation of newly built hydropower reservoirs.

For newly built hydropower reservoirs, the inundated land area itself can be directly modeled with digital elevation models.[76,77] In addition, our values do not account for land occupation and hydropower electricity production changes that may occur due to possible precipitation and related hydrological regime changes under different climate change scenarios.[78]

Further LCA does not account for potential positive effects. Therefore, we did not account for potential positive effects of the hydropower reservoirs on limnic and littoral species like fish[79] or water/shore birds.[80] Moreover, we did not assess the habitat quality of the additional water area introduced. Most reservoirs are rather deep and steep water bodies, which may not represent suitable habitat for many species.

Prospective Implementation in LCA. This paper provides important net land occupation parameters for Norway. Due to the fact that the GLS-1975 data set has a global coverage,[50] our proposed method has the potential to assess the land occupation of storage hydropower reservoirs systematic and with spatial variation on a global scale. In addition, the reservoir filling has an impact beyond the LULUC cause-effect pathways as the increased water surface area of the filled reservoirs leads to consumptive water use through increased evaporation from the open water surface. This is causing potential impacts for aquatic ecosystems by decreasing the discharge.[81] Furthermore, the hydropower reservoirs creation can lead to increased greenhouse gas emissions, which arise from the decomposition of organic matter that was either flooded during reservoir filling or flushed into to the reservoir by river runoff or deposed on the reservoir surface after filling.[29,36,82,83] Therefore, our inundated land area values can be further used to calculate net water consumption and net greenhouse gas emission for the LCI.[27] This is the basis to support the development of methods for assessing the land occupation, water consumption, and greenhouse gas emission impacts of hydropower on biodiversity in LCIA at a damage level, as general applicable LCIA methodology for each of these LCI parameters exists.[81,84,85] With reservoir-specific values we are in addition providing the smallest possible resolution. This enhances the development of needed spatially differentiated LCIA methods.[86,87]

When the application of the land occupation values requires a broader spatial resolution for biodiversity life cycle impact assessment we recommend an aggregation on terrestrial ecoregions for land occupation,[88] for water consumption on freshwater ecoregions[89] and for greenhouse gas emissions on a country level. Furthermore, it highlights once again the importance and possibilities of remote sensing data to improve the LCI and LCIA framework spatially.[90]

Further Application Outside LCA. In this study we used the inundated land area of storage hydropower reservoirs, to calculate inventory parameters suitable for LCA, due to its suitability for identifying potential trade-offs between impact pathways.[21] Indeed, LCA is only one application. The ILA values could also be made publically available by integration in the Global Reservoir and Dam Database.[91] Then the ILA values could be, for example, directly used to assess terrestrial biodiversity impacts of hydropower reservoir inundation.[14,92]

■ ASSOCIATED CONTENT

Supporting Information

The Supporting Information is available free of charge on the ACS Publications website at DOI: 10.1021/acs.est.7b05125.

Details on the case study area and remote sensing data is available as PDF (PDF)

Inventory calculations results are available as Excel file (XLSX)

■ AUTHOR INFORMATION

Corresponding Author

*Phone: +47 73598946; e-mail: martin.dorber@ntnu.no.

ORCID

Martin Dorber: 0000-0001-8477-1934

DOI: 10.1021/acs.est.7b05125
Environ. Sci. Technol. 2018, 52, 2375−2384

Author Contributions

M.D. designed and carried out the analyses. M.D., R.M., and F.V. wrote the manuscript. M.D. made all the figure and tables. All authors have given approval to the final version of the manuscript.

Notes

The authors declare no competing financial interest.

■ ACKNOWLEDGMENTS

We thank John Sebastian Woods for helpful comments and discussions, and Sajith Vezhapparambu for comments on image classification methods. Further, we thank the four anonymous reviewers for their helpful comments. This work was funded by the Research Council of Norway through the SURE project (Project Number 244109)

■ REFERENCES

(1) Moomow, W.; Yamba, F.; Kamimoto, M.; Maurice, L.; Nyboer, J.; Urama, K.; Weir, T., Introduction. In *IPCC Special Report on Renewable Energy Sources and Climate change Mitigation*; Edenhofer, O.; Pichs-Madruga, R.; Sokona, Y.; Seyboth, K.; Matschoss, P.; Kadner, S.; Zwickel, T.; Eickemeier, P.; Hansen, G.; Schlömer, S.; von Stechow, C., Eds.; Cambridge University Press: United Kingdom and New York, NY, 2011.

(2) United Nations *Global Sustainable Development Report*, New York, 2016.

(3) Allison, T. D.; Root, T. L.; Frumhoff, P. C. Thinking globally and siting locally − renewable energy and biodiversity in a rapidly warming world. *Clim. Change* **2014**, *126* (1−2), 1−6.

(4) Jackson, A. L. R. Renewable energy vs. biodiversity: Policy conflicts and the future of nature conservation. *Global Environmental Change* **2011**, *21* (4), 1195−1208.

(5) Santangeli, A.; Toivonen, T.; Pouzols, F. M.; Pogson, M.; Hastings, A.; Smith, P.; Moilanen, A. Global change synergies and trade-offs between renewable energy and biodiversity. *GCB Bioenergy* **2016**, *8* (5), 941−951.

(6) Brown, A.; Muller, S.; Dobrotkova, Z. *Renewable Energy Prospects and Technology*; IEA, 2011.

(7) Kumar, A.; Schei, T.; Ahenkorah, A.; Rodriguez, R. C.; Devernay, J.-M.; Freitas, M.; Hall, D.; Killingtveit, Å.; Liu, Z., Hydropower. In *IPCC Special Report on Renewable Energy Sources and Climate Change Mitigation*; Edenhofer, O.; Pichs-Madruga, R.; Sokona, Y.; Seyboth, K.; Matschoss, P.; Kadner, S.; Zwickel, T.; Eickemeier, P.; Hansen, G.; Schlömer, S.; von Stechow, C., Eds.; Cambridge University Press: Cambridge, United Kingdom and New York, NY, USA, 2011.

(8) Gracey, E. O.; Verones, F. Impacts from hydropower production on biodiversity in an LCA framework—review and recommendations. *Int. J. Life Cycle Assess.* **2016**, *21* (3), 412−428.

(9) Poff, N. L.; Zimmerman, J. K. H. Ecological responses to altered flow regimes: a literature review to inform the science and management of environmental flows. *Freshwater Biol.* **2010**, *55* (1), 194−205.

(10) Crook, D. A.; Lowe, W. H.; Allendorf, F. W.; Eros, T.; Finn, D. S.; Gillanders, B. M.; Hadweng, W. L.; Harrod, C.; Hermoso, V.; Jennings, S.; Kilada, R. W.; Nagelkerken, I.; Hansen, M. M.; Page, T. J.; Riginos, C.; Fry, B.; Hughes, J. M. Human effects on ecological connectivity in aquatic ecosystems: Integrating scientific approaches to support management and mitigation. *Sci. Total Environ.* **2015**, *534*, 52−64.

(11) Jansson, R.; Nilsson, C.; Renofalt, B. Fragmentation of Riparian Floras in Rivers with Multiple Dams. *Ecology* **2000**, *81* (4), 899.

(12) Donaldson, M. R.; Cooke, S. J.; Patterson, D. A.; Macdonald, J. S. Cold shock and fish. *J. Fish Biol.* **2008**, *73* (7), 1491−1530.

(13) Alho, C. J. Environmental effects of hydropower reservoirs on wild mammals and freshwater turtles in Amazonia: a review. *Oecologia Australis* **2011**, *15* (3), 593−604.

(14) Kitzes, J.; Shirley, R. Estimating biodiversity impacts without field surveys: A case study in northern Borneo. *Ambio* **2016**, *45* (1), 110−119.

(15) Zhang, J.; Zhengjun, L.; Xiaoxia, S. Changing landscape in the Three Gorges Reservoir Area of Yangtze River from 1977 to 2005: Land use/land cover, vegetation cover changes estimated using multi-source satellite data. *ITC J.* **2009**, *11* (6), 403−412.

(16) Tefera, B.; Sterk, G. Hydropower-Induced Land Use Change in Fincha'a Watershed, Western Ethiopia: Analysis and Impacts. *Mountain Research and Development* **2008**, *28* (1), 72−80.

(17) McAllister, D. E.; Craig, J. F.; Davidson, N.; Delany, S.; Seddon, M. *Biodiversity Impacts of Large Dams*, 2001.

(18) Egré, D.; Milewski, J. C. The diversity of hydropower projects. *Energy Policy* **2002**, *30* (14), 1225−1230.

(19) Arthington, A. H.; Naiman, R. J.; McClain, M. E.; Nilsson, C. Preserving the biodiversity and ecological services of rivers: new challenges and research opportunities. *Freshwater Biol.* **2010**, *55* (1), 1−16.

(20) Norwegian Government Ministries and Offices, Meld. St. Twenty-five (2015−2016) Power to Change - Energy policy 2030 (In Norwegian).

(21) ISO Environmental management. *Life Cycle Assessment — Principles and Framework*; International Organisation for Standardization: Geneva, Switzerland, 2006.

(22) Duraiappah, A.; Naeem, S.; Agardi, T.; Ash, N.; Cooper, D.; Díaz, S.; Faith, D.; Mace, G.; McNeilly, J.; Mooney, H. Ecosystems and Human Well-Being: Biodiversity Synthesis; World Resources Institute: Washington, DC, 2005; Vol. *86*.

(23) Newbold, T.; Hudson, L. N.; Hill, S. L. L.; Contu, S.; Lysenko, I.; Senior, R. A.; Borger, L.; Bennett, D. J.; Choimes, A.; Collen, B.; Day, J.; De Palma, A.; Diaz, S.; Echeverria-Londono, S.; Edgar, M. J.; Feldman, A.; Garon, M.; Harrison, M. L. K.; Alhusseini, T.; Ingram, D. J.; Itescu, Y.; Kattge, J.; Kemp, V.; Kirkpatrick, L.; Kleyer, M.; Correia, D. L. P.; Martin, C. D.; Meiri, S.; Novosolov, M.; Pan, Y.; Phillips, H. R. P.; Purves, D. W.; Robinson, A.; Simpson, J.; Tuck, S. L.; Weiher, E.; White, H. J.; Ewers, R. M.; Mace, G. M.; Scharlemann, J. P. W.; Purvis, A. Global effects of land use on local terrestrial biodiversity. *Nature* **2015**, *520* (7545), 45−50.

(24) Sala, O. E.; Chapin, F. S.; Armesto, J. J.; Berlow, E.; Bloomfield, J.; Dirzo, R.; Huber-Sanwald, E.; Huenneke, L. F.; Jackson, R. B.; Kinzig, A.; Leemans, R.; Lodge, D. M.; Mooney, H. A.; Oesterheld, M.; Poff, N. L.; Sykes, M. T.; Walker, B. H.; Walker, M.; Wall, D. H. Biodiversity - Global biodiversity scenarios for the year 2100. *Science* **2000**, *287* (5459), 1770−1774.

(25) Gundula, S. B.; Roel, M.; Kjetil, B.; Sigbjorn, S.; Eivin, R. The effects of power lines on ungulates and implications for power line routing and rights-of-way management. *International Journal of Biodiversity and Conservation* **2014**, *6* (9), 647−662.

(26) Rebitzer, G.; Ekvall, T.; Frischknecht, R.; Hunkeler, D.; Norris, G.; Rydberg, T.; Schmidt, W.-P.; Suh, S.; Weidema, B. P.; Pennington, D. W. Life cycle assessment: Part 1: Framework, goal and scope definition, inventory analysis, and applications. *Environ. Int.* **2004**, *30* (5), 701−720.

(27) Flury, K.; Frischknecht, R. Life cycle inventories of hydroelectric power generation. *ESU-Services Ltd* **2012**, 1−51.

(28) Bakken, T. H.; Killingtveit, Å.; Engeland, K.; Alfredsen, K.; Harby, A. Water consumption from hydropower plants - review of published estimates and an assessment of the concept. *Hydrol. Earth Syst. Sci.* **2013**, *17* (10), 3983−4000.

(29) Deemer, B. R.; Harrison, J. A.; Li, S.; Beaulieu, J. J.; DelSontro, T.; Barros, N.; Bezerra-Neto, J. F.; Powers, S. M.; dos Santos, M. A.; Vonk, J. A. Greenhouse Gas Emissions from Reservoir Water Surfaces: A New Global Synthesis. *BioScience* **2016**, *66* (11), 949−964.

(30) Mutel, C. L.; Hellweg, S. Regionalized life cycle assessment: computational methodology and application to inventory databases. *Environ. Sci. Technol.* **2009**, *43* (15), 5797−5803.

(31) Mutel, C. L.; Pfister, S.; Hellweg, S. GIS-Based Regionalized Life Cycle Assessment: How Big Is Small Enough? Methodology and Case

DOI: 10.1021/acs.est.7b05125
Environ. Sci. Technol. 2018, 52, 2375−2384

Study of Electricity Generation. *Environ. Sci. Technol.* **2012**, *46* (2), 1096−1103.
(32) Wernet, G.; Bauer, C.; Steubing, B.; Reinhard, J.; Moreno-Ruiz, E.; Weidema, B. The ecoinvent database version 3 (part I): overview and methodology. *Int. J. Life Cycle Assess.* **2016**, *21* (9), 1218−1230.
(33) Manzano-Agugliaro, F.; Alcayde, A.; Montoya, F. G.; Zapata-Sierra, A.; Gil, C. Scientific production of renewable energies worldwide: An overview. *Renewable Sustainable Energy Rev.* **2013**, *18*, 134−143.
(34) The Ministry of Petroleum and Energy Facts 2015-Energy and Water Resources in Norway 2015.
(35) Scherer, L.; Pfister, S. Global water footprint assessment of hydropower. *Renewable Energy* **2016**, *99*, 711−720.
(36) Scherer, L.; Pfister, S. Hydropower's Biogenic Carbon Footprint. *PLoS One* **2016**, *11* (9), No. e0161947.
(37) Rørslett, B. An integrated approach to hydropower impact assessment. I. Environmental features of some Norwegian hydro-electric lakes. *Hydrobiologia* **1988**, *164* (1), 39−66.
(38) NVE (The Norwegian Water Resources and Energy Directorate). NVE Atlas (15.03.2016); http://atlas.nve.no.
(39) Gao, H.; Birkett, C.; Lettenmaier, D. P., Global monitoring of large reservoir storage from satellite remote sensing. *Water Resour. Res.* **2012**, *48*, (9).10.1029/2012WR012063
(40) Ozesmi, S. L.; Bauer, M. E. Satellite remote sensing of wetlands. *Wetlands Ecol. Manage.* **2002**, *10* (5), 381−402.
(41) Xie, C.; Huang, X.; Mu, H.; Yin, W. Impacts of Land-Use Changes on the Lakes across the Yangtze Floodplain in China. *Environ. Sci. Technol.* **2017**, *51* (7), 3669−3677.
(42) Liu, H.; Yin, Y.; Piao, S.; Zhao, F.; Engels, M.; Ciais, P. Disappearing lakes in semiarid northern China: drivers and environmental impact. *Environ. Sci. Technol.* **2013**, *47* (21), 12107−12114.
(43) Richards, J. A., Remote sensing digital image analysis - An Introduction. *Springer*: **2013**; *Vol. 5*.10.1007/978-3-642-30062-2
(44) USGS (United States Geological Survey). EarthExplorer-Global Land Survey 1975 dataset (01.05.2016); http://earthexplorer.usgs.gov/.
(45) Geodata, A. S. NORGE i Bilder - Image search (01.05.2016); https://www.norgeibilder.no/.
(46) Zohary, T.; Ostrovsky, I. Ecological impacts of excessive water level fluctuations in stratified freshwater lakes. *Inland Waters* **2011**, *1* (1), 47−59.
(47) Giri, C.; Ochieng, E.; Tieszen, L. L.; Zhu, Z.; Singh, A.; Loveland, T.; Masek, J.; Duke, N. Status and distribution of mangrove forests of the world using earth observation satellite data. *Global Ecology and Biogeography* **2011**, *20* (1), 154−159.
(48) Butera, M. K. Remote sensing of wetlands. *IEEE Transactions on Geoscience and Remote Sensing* **1983**, *3*, 383−392.
(49) Smith, L. C. Satellite remote sensing of river inundation area, stage, and discharge: A review. *Hydrol. Processes* **1997**, *11* (10), 1427−1439.
(50) Gutman, G.; Huang, C.; Chander, G.; Noojipady, P.; Masek, J. G. Assessment of the NASA−USGS Global Land Survey (GLS) datasets. *Remote Sensing of Environment* **2013**, *134*, 249−265.
(51) *ArcGIS Release 10.3*; ESRI (Environmental Systems Research Institute): Redlands, CA, 2014.
(52) Milà i Canals, L.; Bauer, C.; Depestele, J.; Dubreuil, A.; Freiermuth Knuchel, R.; Gaillard, G.; Michelsen, O.; Müller-Wenk, R.; Rydgren, B. Key Elements in a Framework for Land Use Impact Assessment Within LCA (11 pp). *Int. J. Life Cycle Assess.* **2007**, *12* (1), 5−15.
(53) Bednarek, A. T. Undamming Rivers: A Review of the Ecological Impacts of Dam Removal. *Environ. Manage.* **2001**, *27* (6), 803−814.
(54) East, A. E.; Pess, G. R.; Bountry, J. A.; Magirl, C. S.; Ritchie, A. C.; Logan, J. B.; Randle, T. J.; Mastin, M. C.; Minear, J. T.; Duda, J. J.; Liermann, M. C.; McHenry, M. L.; Beechie, T. J.; Shafroth, P. B. Large-Scale Dam Removal on the Elwha River River Channel and Floodplain Geomorphic Change. *Geomorphology*, Washington, U.S., 2015, *228*, 765−786.
(55) NVE (The Norwegian Water Resources and Energy Directorate). Vannkraftdatabase (20.11.2017); https://www.nve.no/energiforsyning-og-konsesjon/vannkraft/vannkraftdatabase.
(56) Rehman, S.; Al-Hadhrami, L. M.; Alam, M. M. Pumped hydro energy storage system: A technological review. *Renewable Sustainable Energy Rev.* **2015**, *44*, 586−598.
(57) Frazier, P. S.; Page, K. J. Water body detection and delineation with Landsat TM data. *Photogrammetric Engineering and Remote Sensing* **2000**, *66* (12), 1461−1468.
(58) Thematic Mapping API. World Borders Dataset (11.04.2016); http://thematicmapping.org/downloads/world_borders.php.
(59) McFeeters, S. K. The use of the Normalized Difference Water Index (NDWI) in the delineation of open water features. *International journal of remote sensing* **1996**, *17* (7), 1425−1432.
(60) Ji, L.; Zhang, L.; Wylie, B. Analysis of dynamic thresholds for the normalized difference water index. *Photogrammetric Engineering & Remote Sensing* **2009**, *75* (11), 1307−1317.
(61) Xu, H. Modification of normalised difference water index (NDWI) to enhance open water features in remotely sensed imagery. *International Journal of Remote Sensing* **2006**, *27* (14), 3025−3033.
(62) Sobek, S.; Nisell, J.; Fölster, J. Predicting the volume and depth of lakes from map-derived parameters. *Inland Waters* **2011**, *1* (3), 177−184.
(63) NVE (The Norwegian Water Resources and Energy Directorate). Dybdekart over norske innsjøer 1984 (In Norwegian with English summary) (01.06.2016); https://gis3.nve.no/metadata/tema/DKBok1984/Dybdekart_1984.htm.
(64) Kartverket. Historia om Noreg 1:50 000 (07.08.2017); http://www.kartverket.no/Kunnskap/Historie/Historien-om-Norge-1-50-000/.
(65) Hertwich, E. G.; Gibon, T.; Bouman, E. A.; Arvesen, A.; Suh, S.; Heath, G. A.; Bergesen, J. D.; Ramirez, A.; Vega, M. I.; Shi, L. Integrated life-cycle assessment of electricity-supply scenarios confirms global environmental benefit of low-carbon technologies. *Proc. Natl. Acad. Sci. U. S. A.* **2015**, *112* (20), 6277−6282.
(66) Denholm, P.; Hand, M.; Jackson, M.; Ong, S. *Land-Use Requirements of Modern Wind Power Plants in the United States*; National Renewable Energy Laboratory: Golden, Colorado, **2009**; 10.2172/964608
(67) Fthenakis, V.; Kim, H. C. Land use and electricity generation: A life-cycle analysis. *Renewable Sustainable Energy Rev.* **2009**, *13* (6−7), 1465−1474.
(68) Bakken, T. H.; Modahl, I. S.; Raadal, H. L.; Bustos, A. A.; Arnoy, S. Allocation of water consumption in multipurpose reservoirs. *Water Policy* **2016**, *18* (4), 932−947.
(69) Zlinszky, A.; Heilmeier, H.; Balzter, H.; Czúcz, B.; Pfeifer, N. Remote Sensing and GIS for Habitat Quality Monitoring: New Approaches and Future Research. *Remote Sensing* **2015**, *7* (6), 7987−7994.
(70) Hofmann, H.; Lorke, A.; Peeters, F. Temporal scales of water-level fluctuations in lakes and their ecological implications. *Hydrobiologia* **2008**, *613* (1), 85−96.
(71) Wantzen, K. M.; Rothhaupt, K.-O.; Mörtl, M.; Cantonati, M.; G.-Tóth, L.; Fischer, P. Ecological effects of water-level fluctuations in lakes: an urgent issue. *Hydrobiologia* **2008**, *613* (1), 1−4.
(72) Evtimova, V. V.; Donohue, I. Water-level fluctuations regulate the structure and functioning of natural lakes. *Freshwater Biol.* **2016**, *61* (2), 251−264.
(73) Mjelde, M.; Hellsten, S.; Ecke, F. A water level drawdown index for aquatic macrophytes in Nordic lakes. *Hydrobiologia* **2013**, *704* (1), 141−151.
(74) Koellner, T.; de Baan, L.; Beck, T.; Brandão, M.; Civit, B.; Margni, M.; i Canals, L. M.; Saad, R.; de Souza, D. M.; Müller-Wenk, R. UNEP-SETAC guideline on global land use impact assessment on biodiversity and ecosystem services in LCA. *Int. J. Life Cycle Assess.* **2013**, *18* (6), 1188−1202.
(75) Koellner, T.; de Baan, L.; Beck, T.; Brandão, M.; Civit, B.; Goedkoop, M.; Margni, M.; Milà i Canals, L.; Müller-Wenk, R.;

DOI: 10.1021/acs.est.7b05125
Environ. Sci. Technol. 2018, 52, 2375−2384

Weidema, B.; Wittstock, B. Principles for life cycle inventories of land use on a global scale. *Int. J. Life Cycle Assess.* **2013**, *18* (6), 1203−1215.
(76) Merwade, V.; Cook, A.; Coonrod, J. GIS techniques for creating river terrain models for hydrodynamic modeling and flood inundation mapping. *Environmental Modelling & Software* **2008**, *23* (10−11), 1300−1311.
(77) Wang, Y.; Liao, M.; Sun, G.; Gong, J. Analysis of the water volume, length, total area and inundated area of the Three Gorges Reservoir, China using the SRTM DEM data. *International Journal of Remote Sensing* **2005**, *26* (18), 4001−4012.
(78) Hanafiah, M. M.; Xenopoulos, M. A.; Pfister, S.; Leuven, R. S. E. W.; Huijbregts, M. A. J. Characterization Factors for Water Consumption and Greenhouse Gas Emissions Based on Freshwater Fish Species Extinction. *Environ. Sci. Technol.* **2011**, *45* (12), 5272−5278.
(79) Lehtonen, H.; Rask, M.; Pakkasmaa, S.; Hesthagen, T. Freshwater fishes, their biodiversity, habitats and fisheries in the Nordic countries. *Aquat. Ecosyst. Health Manage.* **2008**, *11* (3), 298−309.
(80) Jonsson, M.; Strasevicius, D.; Malmqvist, B. Influences of river regulation and environmental variables on upland bird assemblages in northern Sweden. *Ecol. Res.* **2012**, *27* (5), 945−954.
(81) Tendall, D. M.; Hellweg, S.; Pfister, S.; Huijbregts, M. A. J.; Gaillard, G. Impacts of River Water Consumption on Aquatic Biodiversity in Life Cycle Assessment—A Proposed Method, and a Case Study for Europe. *Environ. Sci. Technol.* **2014**, *48* (6), 3236−3244.
(82) Abril, G.; Guérin, F.; Richard, S.; Delmas, R.; Galy-Lacaux, C.; Gosse, P.; Tremblay, A.; Varfalvy, L.; Dos Santos, M. A.; Matvienko, B. Carbon dioxide and methane emissions and the carbon budget of a 10-year old tropical reservoir (Petit Saut, French Guiana). *Global Biogeochemical Cycles* **2005**, *19* (4), n/a.
(83) DelSontro, T.; McGinnis, D. F.; Sobek, S.; Ostrovsky, I.; Wehrli, B. Extreme Methane Emissions from a Swiss Hydropower Reservoir: Contribution from Bubbling Sediments. *Environ. Sci. Technol.* **2010**, *44* (7), 2419−2425.
(84) Chaudhary, A.; Verones, F.; de Baan, L.; Hellweg, S. Quantifying Land Use Impacts on Biodiversity: Combining Species−Area Models and Vulnerability Indicators. *Environ. Sci. Technol.* **2015**, *49* (16), 9987−9995.
(85) De Schryver, A. M.; Brakkee, K. W.; Goedkoop, M. J.; Huijbregts, M. A. J. Characterization Factors for Global Warming in Life Cycle Assessment Based on Damages to Humans and Ecosystems. *Environ. Sci. Technol.* **2009**, *43* (6), 1689−1695.
(86) Rugani, B.; Rocchini, D. Boosting the use of spectral heterogeneity in the impact assessment of agricultural land use on biodiversity. *J. Cleaner Prod.* **2017**, *140*, 516−524.
(87) Curran, M.; Maia de Souza, D.; Antón, A.; Teixeira, R. F. M.; Michelsen, O.; Vidal-Legaz, B.; Sala, S.; Milà i Canals, L. How Well Does LCA Model Land Use Impacts on Biodiversity?—A Comparison with Approaches from Ecology and Conservation. *Environ. Sci. Technol.* **2016**, *50* (6), 2782−2795.
(88) Olson, D. M.; Dinerstein, E.; Wikramanayake, E. D.; Burgess, N. D.; Powell, G. V. N.; Underwood, E. C.; D'Amico, J. A.; Itoua, I.; Strand, H. E.; Morrison, J. C.; Loucks, C. J.; Allnutt, T. F.; Ricketts, T. H.; Kura, Y.; Lamoreux, J. F.; Wettengel, W. W.; Hedao, P.; Kassem, K. R. Terrestrial Ecoregions of the World: A New Map of Life on Earth. *BioScience* **2001**, *51* (11), 933.
(89) Abell, R.; Thieme, M. L.; Revenga, C.; Bryer, M.; Kottelat, M.; Bogutskaya, N.; Coad, B.; Mandrak, N.; Balderas, S. C.; Bussing, W.; Stiassny, M. L. J.; Skelton, P.; Allen, G. R.; Unmack, P.; Naseka, A.; Ng, R.; Sindorf, N.; Robertson, J.; Armijo, E.; Higgins, J. V.; Heibel, T. J.; Wikramanayake, E.; Olson, D.; López, H. L.; Reis, R. E.; Lundberg, J. G.; Sabaj Pérez, M. H.; Petry, P. Freshwater Ecoregions of the World: A New Map of Biogeographic Units for Freshwater Biodiversity Conservation. *BioScience* **2008**, *58* (5), 403.
(90) Abotalib, M.; Zhao, F.; Clarens, A. Deployment of a Geographical Information System Life Cycle Assessment Integrated Framework for Exploring the Opportunities and Challenges of Enhanced Oil Recovery Using Industrial CO2Supply in the United States. *ACS Sustainable Chem. Eng.* **2016**, *4* (9), 4743−4751.
(91) Fluet-Chouinard, E.; Lehner, B.; Rebelo, L.-M.; Papa, F.; Hamilton, S. K. Development of a global inundation map at high spatial resolution from topographic downscaling of coarse-scale remote sensing data. *Remote Sensing of Environment* **2015**, *158*, 348−361.
(92) Pandit, M. K.; Grumbine, R. E. Potential Effects of Ongoing and Proposed Hydropower Development on Terrestrial Biological Diversity in the Indian Himalaya. *Conservation Biology* **2012**, *26* (6), 1061−1071.

DOI: 10.1021/acs.est.7b05125
Environ. Sci. Technol. 2018, 52, 2375−2384